Solid State Dehydration Processes: Mechanism of Water Loss from Crystalline Inosine Dihydrate

Amy L. Gillon,[†,||] Roger J. Davey*[,†] Richard Storey[‡,⊥] Neil Feeder[‡], Gary Nichols[‡], Geoffrey Dent[†], and David C. Apperley[§]

The Molecular Materials Centre, School of Chemical Engineering and Analytical Sciences, University of Manchester, P. O. Box 88, Manchester, M60 1QD, United Kingdom, Pharmaceutical R&D, Pfizer Global R&D, Sandwich, Kent, CT13 9NJ, United Kingdom, and Industrial Research Laboratories, University of Durham, Durham, DH1 3HP, United Kingdom

Received: August 27, 2004; In Final Form: January 17, 2005

The solid state dehydration of inosine dihydrate has been investigated using powder X-ray diffraction, differential scanning calorimetry, thermal gravimetric analysis, dynamic vapor sorption, hot stage microscopy, ^{13}C solid state NMR, and variable temperature Fourier transform infrared spectroscopy. The information obtained from these experiments has been combined with an analysis of the crystallographic packing of inosine dihydrate and its two anhydrous polymorphs to yield mechanistic insights into the modes of water loss. The results allow an understanding of why, surprisingly, the dehydration of the dihydrate is always found to give the anhydrous, metastable, α-form.

Introduction

Polymorphism and solvate formation are problems that are commonly encountered in the processing of pharmaceutical solids. Of the solvents regularly used for crystallization, water is most commonly incorporated into the solid state to form hydrates. This results from its small size and hydrogen bonding capability, and it is thought that approximately one-third of pharmaceuticals are capable of forming hydrates.[1] Our recent study of the Cambridge Structural Database (CSD) revealed that between 3000 and 4000 structures of organic molecules are hydrated.[2] The formation of hydrates and their potential to transform to anhydrous structures can affect various pharmaceutically important physicochemical properties including stability, solubility, dissolution rate, bioavailability, compactability, and tableting behavior. Three cases of dehydration in the solid state have been distinguished, in which (a) the anhydrous crystal lattice is nearly identical to that of the original hydrate, (b) the residue is poorly crystalline or amorphous, and (c) the residue crystallizes with a different crystal lattice.[3] Various studies have been reported on the dehydration behavior of hydrates, including carbamazepine dihydrate,[4] cromolyn sodium hydrates,[5] and aspartame hemihydrate.[6] The majority of these studies, however, deal with "isomorphous" systems in which the hydrate and the anhydrous structure are very similar, water molecules are lost through channels within the structure,[7] and the dehydration process is reversible.[8] Typical examples of such materials are caffeine, theophylline, and thiamine hydrochloride.[9−11] There appears to be a lack of knowledge and understanding of the structural changes that accompany more complex dehydrations in which there are, for example, multiple sites from which water must be lost, a significant structural rearrangement, and no evidence of reversibility. Recent work on the dehydration of trehalose[12] and the copper salt of 8-hydroxyquinolate[13] to either amorphous or polymorphic modifications is indicative of such complexity and illustrative of the application of various kinetic measurements to yield insight into the controlling parameters. Our contribution extends such an approach: we report on the solid state dehydration of the complex dihydrate of inosine and show how a range of analytical techniques can be used to elucidate structural insights into the transformation process. In particular, we are able to provide insight into why the dehydration proceeds to the metastable, α, polymorph rather than the stable, structurally related *β*-form.

Inosine, Figure 1a, is a nucleoside closely related to adenosine. It is a constituent of ribonucleic acids, and is found particularly in transfer RNA. It has two known anhydrous polymorphs (α and *β*) and a dihydrate. It has been chosen for this work because the crystal structures of these three forms are known[14−16] and solubility data for each form in water have been reported.[17] The *β*-form is more stable than the α-form at all temperatures, while in aqueous slurries at temperatures between 10 and 18 °C the dihydrate is more stable than the α-form, but less stable than the *β*-form. Below 10 °C, the dihydrate is the most stable form.

Crystal Structures

The crystal structures of each of the three forms were studied to compare the conformations of the inosine molecules and their packing. The crystallographic information and graph set analyses can be seen in Tables 1 and 2, respectively. For graph set analyses the letters "C", "D", and "S" are used to describe hydrogen bond motifs. C*x*,*y*(*z*) describes a chain with *x* hydrogen bond donors, *y* hydrogen bond acceptors, and *z* atoms in the chain. In similar notation "D" represents a dimer hydrogen bond and "S" an intramolecular hydrogen bond.[18,19]

Among the three crystalline forms there are five independent conformations of the inosine molecule. The torsion angles of the N−C bond connecting the aromatic ring to the furan ring (C2−N−C6−C7, in Figure 1a) are as follows: α-form 60.7°, 63.9°, *β*-form 68.4°, dihydrate −174.3°, 110.7°; the conformations can be seen overlaid in Figure 1b.

† University of Manchester.
‡ Pfizer Global R&D.
§ University of Durham.
|| Current address: Pharmaceutical R&D, Pfizer Global R&D, Sandwich, Kent, CT13 9NJ, U.K.
⊥ Current address: AstraZeneca, Silk Road Business Park, Macclesfield, Cheshire, SK10 2NA, U.K.

10.1021/jp046122l CCC: $30.25
Published on Web 02/26/2005

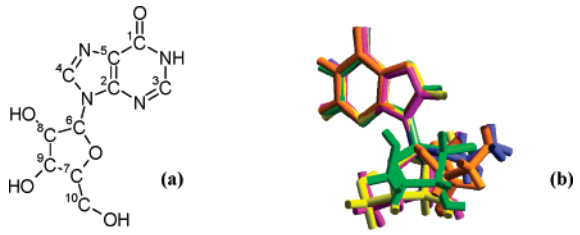

Figure 1. (a) Molecular structure of inosine. (b) Five conformations of inosine: α-form in pink and yellow, *β*-form in blue, and dihydrate form in green and orange.

TABLE 1: Crystal Structure Data

form	α	*β*	dihydrate
crystal system	orthorhombic	monoclinic	monoclinic
space group	*P*212121	*P*21	*P*21
A	13.261(2)	4.818(5)	17.573(1)
B	21.285(2)	10.450(10)	11.278(1)
C	8.097(1)	10.970(10)	6.654(1)
α	90	90	90
β	90	90.72(3)	98.23(1)
γ	90	90	90
volume	2285.462	552.275	1305.164
Z	8	2	4

TABLE 2: Graph Set Analysis

α	*β*	dihydrate
C1,1(5)	2 × C1,1(5)	C1,1(7)
C1,1(10)	C1,1(11)	2 × C1,1(5)
S1,1(9)	C1,1(8)	13 × D1,1(2)
4 × D1,1(2)	S1,1(5)	

There are two independent inosine conformers in the α-form. The structure contains a C1,1(5) chain, shown in Figure 2a, that runs along the *c*-axis and contains only one conformer. The H-bond in this chain, O−H···O, is of length 2.036 Å. There is also a C1,1(10) chain that runs along the *b*-axis, involves the second conformer, and contains an H-bond, O−H···O═C, of length 2.373 Å. Also present in this structure is one intramolecular H-bond (S1,1(9)), O−H···N, of length 2.821 Å in one conformer and 2.341 Å in the other. There are four other dimer interactions (D), between two independent conformers and involving the groups OH···N (1.921, 1.776 Å) and NH···O (2.073, 2.147 Å). The O−H···N interactions lie along the *b*-axis, and the NH···O interactions lie along the *a*-axis.

The *β*-form contains only one conformation of the inosine molecule. There are four H-bonded chains running along the *b*-axis. A C1,1(5) chain, shown in Figure 2b, involves only the aromatic part of the inosine molecule. The H-bond in this chain, N−H···N, is of length 2.146 Å. A second C1,1(5) chain utilizes the O−H···O interaction (2.091 Å) in the nonaromatic part of the inosine molecule. A C1,1(8) chain contains an H-bond, O−H···N, of length 2.063 Å, and a C1,1(11) chain contains an H-bond, O−H···O═C, of length 1.838 Å. The inosine molecule contains an intramolecular H-bond, O−H···O, of length 2.377 Å.

The dihydrate form comprises two conformations of inosine and four independent water molecules. A C1,1(7) chain, shown in Figure 3a, utilizes the O−H···O interaction of length 1.971 Å, contains only one conformer, and runs along the *c*-axis. There are two identical C1,1(5) chains, shown in Figure 3b, running along the *b*-axis, each involving only the aromatic part of the molecule, and each comprising only one of the two conformers. The H-bonds, N−H···N, involved with these chains are of lengths 1.921 and 1.741 Å. There are 13 dimer interactions in this structure, only two of which do not involve a water molecule.

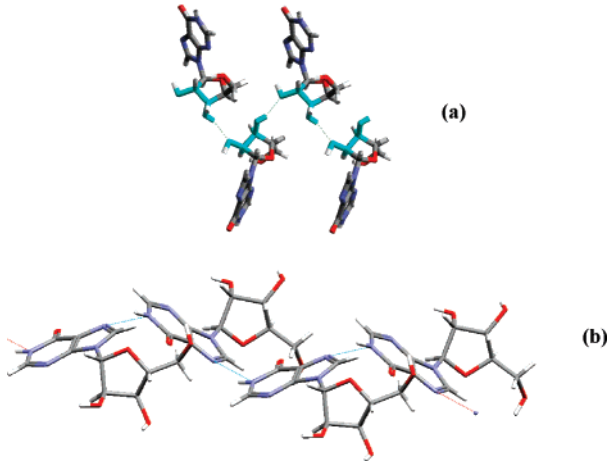

Figure 2. (a) C1,1(5), O−H···O, chain in α-inosine; (b) C1,1(5), N−H···N, chain in *β*-inosine.

Each of the four water molecules have different H-bonding environments, and following our previous classification,[2] three are environment "5" and one is environment "6". They are each involved in hydrogen bonding to both the inosine molecules and other water molecules. These environments are shown schematically in Figure 4. The H-bonds are in molecule (1) H···OH 1.911 Å, H···OH_2 2.198 Å, and O···HO 1.937 Å; in molecule (2) H···O═C 2.055 Å, H···OH_2 2.197 Å, and O···HO 1.829 Å; in molecule (3) H···O═C 2.333 Å, H···OH_2 1.842 Å, and O···H_2O 2.197 Å; and in molecule (4) H···OH 1.901 Å, H···OH 1.897 Å, O···HO 1.968 Å, and O···H_2O 2.198 Å. Two of the water molecules, (1) and (4), are located in the neighborhood of the hydroxyl groups, while the two remaining waters, (2) and (3), lie between aromatic planes. Their structural locations are shown in Figure 3c.

Overall, we note that, while the α- and *β*-polymorphs share a common C1,1(5), O−H···O, chain, the only common element relating the polymorphs to the dihydrate is the C1,1(5), N−H···N, chain that it shares with the *β*-form.

Experimental Section

The (−)-inosine used in all the studies was obtained from Sigma Aldrich (99% purity).The dihydrate was crystallized by crash cooling a saturated aqueous solution prepared from α-inosine from 50 to 5 °C and leaving to stir for 24 h. Solid samples were vacuum filtered, left for 24 h under ambient conditions to dry, and stored in sealed glass vials.

Differential scanning calorimetric (DSC) curves were determined using a TA Instruments Q1000 differential scanning calorimeter, calibrated with indium. Samples (3−9 mg) were heated in closed aluminum pans at 1, 5, 10, 20, 50, and 100 °C/min under nitrogen purge at 50 mL/min from ambient to 300 °C. Thermal gravimetric analytical (TGA) curves were recorded using a TA Instruments Hi-Res TGA 2950 analyzer. Samples (5−9 mg) were heated in open platinum pans at 5 and 10 °C/min with a nitrogen purge at 50 mL/min from ambient temperature to 150 °C.

Moisture absorption/desorption isotherms were collected on a Surface Measurement Systems Ltd. dynamic vapor sorption (DVS) instrument. The data were collected at 30 °C at relative humidities of 0, 15, 30, 45, 60, 75, and 90% relative humidity (RH). The minimum time for each step was 120 min with a stability entry of 0.0003% averaged over 5 min.

Hot stage microscopy (HSM) was carried out using a Mettler FP5 controller and FP52 heating stage mounted on a Nikon

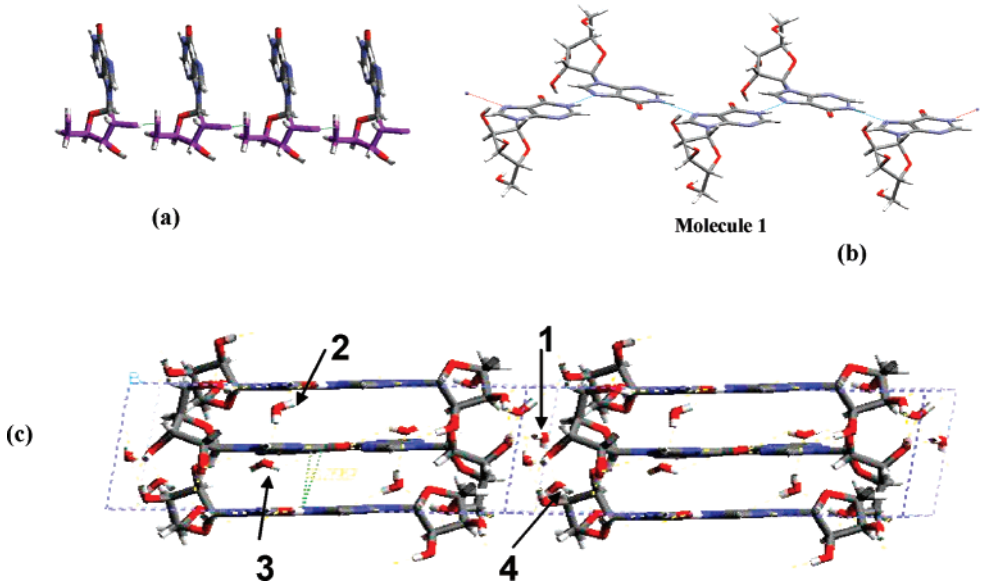

Figure 3. (a) C1,1(7), O−H···O, chain in inosine dihydrate; (b) C1,1(5), N−H···N, chain in inosine dihydrate; (c) water molecule locations in inosine dihydrate, viewed down *b*.

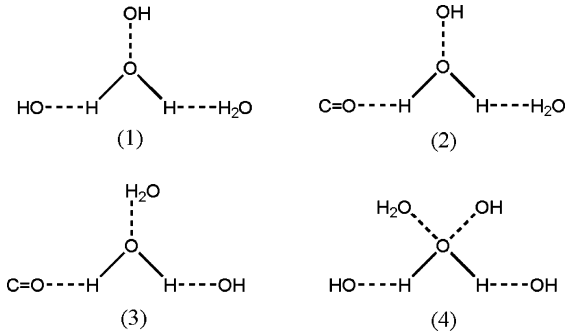

Figure 4. Water molecule environments in inosine dihydrate designated according to Gillon et al.[2]

Optiphot Pol 2 polarizing light microscope. Crystals were examined both dry and dispersed in silicone oil and heated at 10 °C/min.

Variable temperature and humidity powder X-ray diffraction (PXRD) patterns were recorded using a Bruker D8 Advance diffractometer fitted with an environmental chamber. Cu Kα radiation ($\lambda = 1.5406$ Å) was used, and the diffraction angle, 2θ, was scanned from 4° to 35°, with a step size of 0.014°, a step time of 0.3 s, and a delay time of 120 s. For studying the effect of increasing temperature, samples were packed in a copper sample holder and heated in 20 °C steps to set temperatures between 40 and 140 °C. In the variable humidity experiments, the humidity within the environmental chamber was decreased from 45% to 0% RH in 15% steps over a number of hours. The experiment was designed to have 15% RH steps in humidity to correlate to the DVS experiment.

Solid state ^{13}C spectra were obtained using a Varian Unity Inova spectrometer with a 7.5 mm (rotor outside diameter) Varian MAS probe operating at 75.430 MHz. Spectra were obtained using a cross-polarization experiment with radio frequency fields of (frequency equivalent) 60 kHz. The spectrum from the α-form was obtained with a 45 s recycle and 5 ms contact time, that from the β-form with a 90 s recycle and 5 ms contact time, and that from the dihydrate with a 10 s recycle and 1 ms contact time. For the α- and β-forms the sample spin rate was about 5 kHz, and for the dihydrate it was about 3.7 kHz. Spectra were obtained at ambient temperature (about 23 °C) and as a function of temperature, in the range ambient temperature to 60 °C. Temperature calibration was carried out using methanol. Spectral referencing is with respect to tetramethylsilane (carried out indirectly by setting the high-frequency signal from adamantane to 38.4 ppm).

Fourier transform infrared (FT-IR) spectra of inosine dihydrate were collected, between 4000 and 750 cm^{-1}, with a ThermoNicolet Avatar-360 Fourier transform infrared spectrometer equipped with a Golden-Gate accessory sample stage. Spectra were recorded at 10 °C intervals over a temperature range of 23−140 °C.

Cerius[2] (Accelrys, Cambridge, UK) and the CCDC program Mercury were used to visualize crystal structures and to calculate the theoretical X-ray powder patterns. The graph set analysis was performed using the CCDC program R-Pluto.[20]

Results

Thermal Analytical Studies (DSC, TGA, and HSM). In thermal analytical studies the dehydration event can be clearly observed. DSC data, shown in Figure 5, were collected on the dihydrate at a variety of heating rates, and the dehydration event can be seen to commence around 60 °C. It appears to be a two-stage process (with peaks at 69.8 and 79.7 °C), but despite the use of various heating rates it was not possible to separate the two events. Dehydration was also detected over the same temperature range by TGA. The overall weight loss was as expected for a dihydrate, and two, poorly resolved, stages were again observed. It appeared that approximately 80% of the water was lost during the initial stage. This would be consistent with the initial loss of the three of the environment "5" water molecules followed by loss of those in the more tightly bound environment "6" over the remainder of the heating range. Hot stage microscopy revealed the dehydration event as a gradual darkening of the crystals as shown in Figure 6. In agreement with DSC and TGA, dehydration started at 58 °C and was complete by about 70 °C. On cooling to room temperature the dehydrated hydrate crystals were then immersed in silicone oil to reduce contrast. Figure 6d shows a closeup of the rectangular crystal shown at the center of Figure 6a−c. Radiating needlelike crystals have grown within the dehydrated crystal to produce pseudomorphs of the dihydrate.

Powder X-ray Diffraction Studies. One of the most effective ways of studying both thermally and humidity driven dehydra-

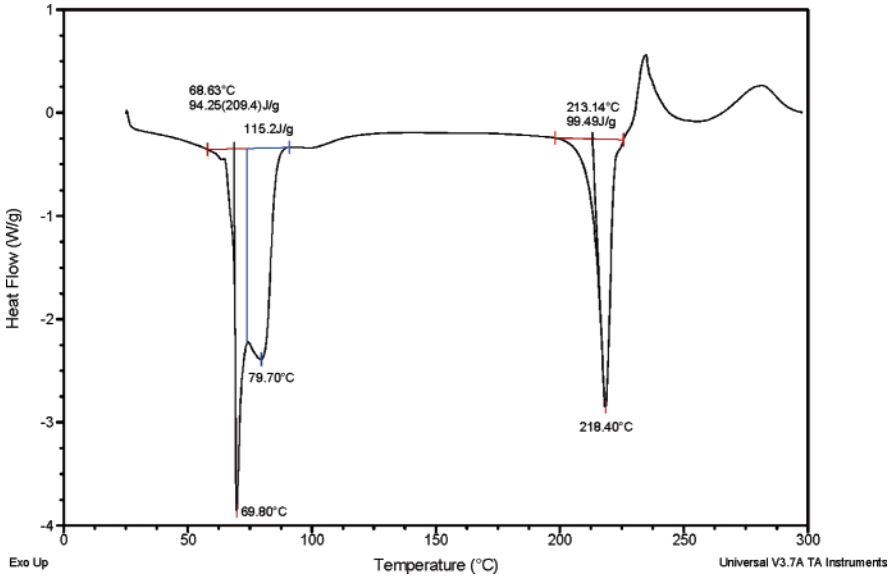

Figure 5. DSC of inosine dihydrate recorded at a heating rate of 10 °C/min.

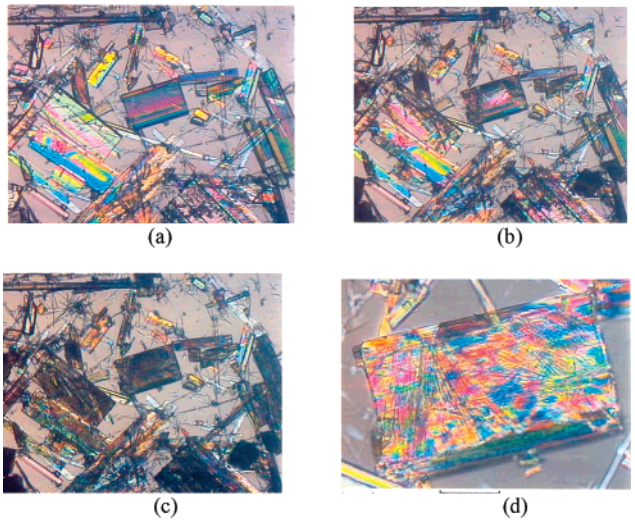

Figure 6. HSM experiment on inosine dihydrate: photographs (a) at 25 °C, (b) at 58 °C, (c) at 70 °C, and (d) cooled to room temperature (in oil). The rectangular crystal in the center of (a)−(c) and magnified in (d) is 200 μm across its diagonal.

tion was with PXRD. From the calculated patterns of each form, characteristic peaks (at 11.760° 2θ in α, 10.654° 2θ in β, and 5.081° 2θ in the dihydrate) for each were identified and followed throughout the dehydration.

The results of the thermal study are shown in Figure 7. A sample of dihydrate was heated in 20 °C steps from room temperature to 140 °C. The first changes are seen in the 60 °C pattern with a new peak appearing at 5.876° and a shoulder evident at 5.327° on the original 5.081° dihydrate peak. This 5.081° reflection corresponds to the (100) layer of the dihydrate structure. Since this is the channel containing waters (1) and (4) (see Figure 3c), the decrease in intensity of this peak at 5.081° and the short-lived appearance of the shoulder imply a contraction of the channel to a smaller *d* spacing as the water is lost. The new peak at 5.876° continues to grow at higher temperatures while the peak at 5.081° decreases, and this may reflect further contraction of the channel. Also, in the pattern collected at 60 °C, two new peaks can be seen at 8.327° and 10.743° 2θ, both corresponding to peaks found in the α-pattern. At 100 °C the pattern contains peaks at 5.876°, 9.697°, and 18.663° that are not found in any of the known forms. By 120 °C the peaks at 5.093° and 9.697° have completely disappeared while the 5.876° and 18.663° peaks remain. On cooling to room temperature, a further peak initially grew at 6.423° 2θ that does not correspond to any peak previously seen, and the final pattern, collected after 1 h at room temperature, corresponded to the α-structure. Overall, these data demonstrate that the dihydrate dehydrates in the solid state, remaining crystalline throughout, to give the anhydrous, metastable, α-form. It is clear from these time-resolved data that, during this process, PXRD patterns are observed over the range 60−140 °C that do not correspond to any of the known forms.

The humidity study involved leaving a sample of dihydrate at room temperature and 45% RH for 17 h and collecting PXRD patterns every hour. After 4 h peaks corresponding to the α-form were observed. After 17 h the humidity was then decreased to 30% RH and patterns were collected over 2 h. Finally, it was dropped to 15% RH and patterns were collected over 14 h. Throughout this experiment there was a mixture of the dihydrate and the α-form with the dihydrate peaks decreasing and the α-peaks increasing in intensity as shown in Figure 8. Unlike the heating experiment described above, no peaks were observed that could not be assigned to either the dihydrate or the α-form.

Spectroscopic Studies. FT-IR spectra of the pure phases at room temperature (not shown) revealed differences in hydrogen bonding at the carbonyl groups of each form, giving rise to distinct changes in the 1650−1750 cm^{-1} region of the spectrum. In the dihydrate there are two peaks at 1686.54 and 1739.03 cm^{-1}. In the α-form, there is a single carbonyl peak (with a small shoulder) at 1687.75 cm^{-1}, while in the β-form there is also a single peak at 1693.31 cm^{-1}. These values are typical for H-bonded carbonyls with the unusually high band in the dihydrate indicating that one of them is very tightly locked into position within the structure.

Other major differences between the three forms were seen in the 3500−3000 cm^{-1} region. The N−H stretch is found at 3307.25 cm^{-1} in the α-form, at 3288.37 cm^{-1} in the β-form, and at 3306.55 cm^{-1} in the dihydrate. In addition, there is an O−H stretch at 3534 cm^{-1} in α, at 3431.19 cm^{-1} in β, and at 3462.30 and 3549.36 cm^{-1} in the dihydrate. These latter two peaks in the dihydrate are characteristic for water bound in the crystalline lattice rather than for water molecules hydrogen bonding to each other.

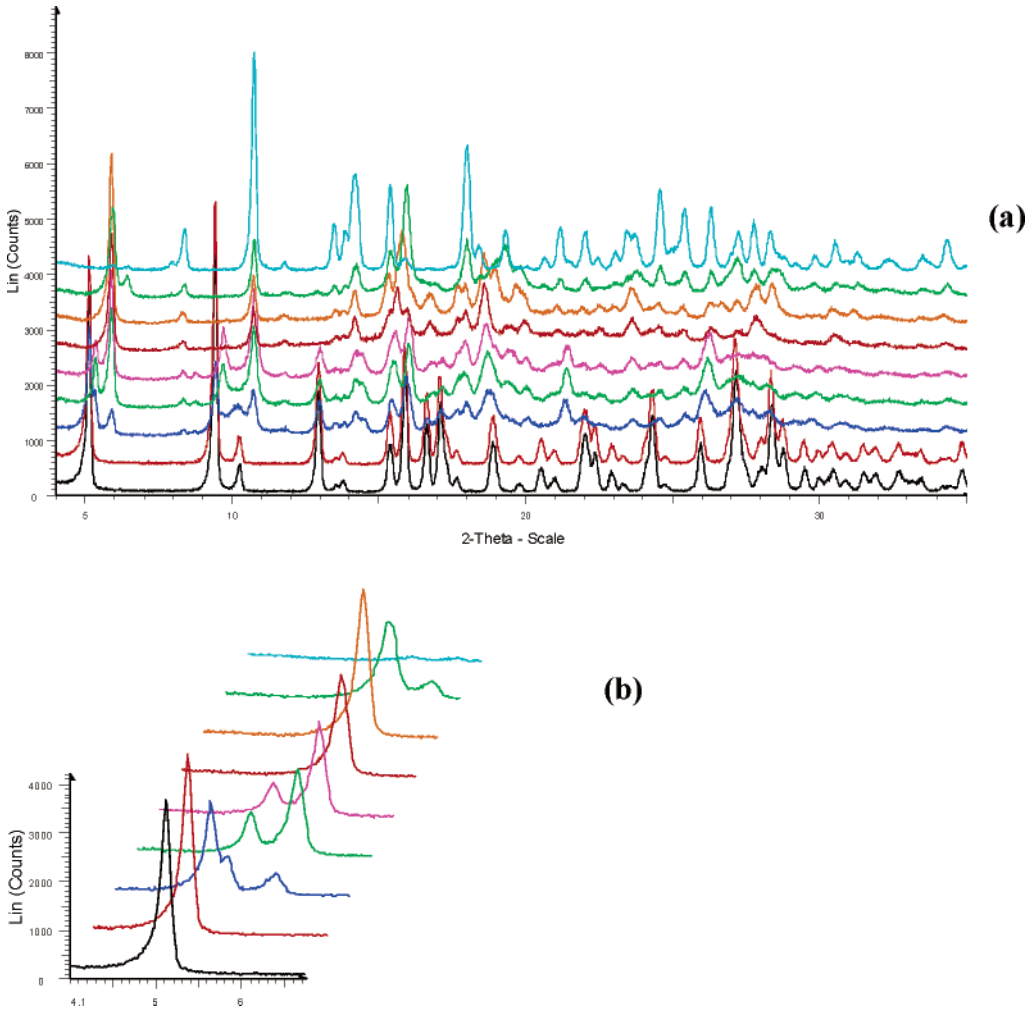

Figure 7. PXRD patterns showing thermal dehydration of inosine dihydrate between 40 and 140 °C (from bottom: room temperature, 40 °C, 60 °C, 80 °C, 100 °C, 120 °C, 140 °C, room temperature, 1 h after cooling). (a) Complete 2θ range; (b) expanded view of low-angle region $4° < 2\theta < 6°$.

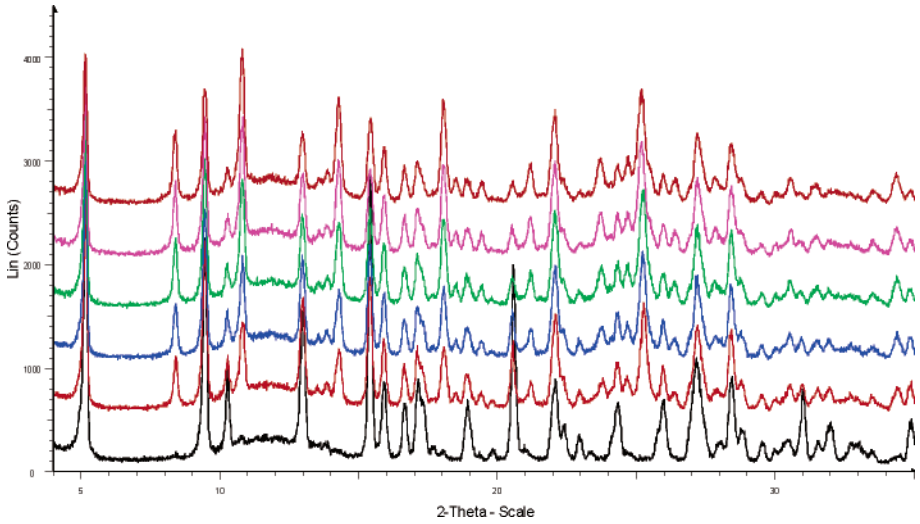

Figure 8. PXRD patterns showing dehydration of inosine dihydrate over relative humidity range 45−15% (from bottom: 45% RH initial, 45% RH final, 30% RH initial, 30% RH final, 15% RH initial, 15% RH final).

Upon heating the dihydrate to 32 °C its characteristic carbonyl stretches are found at 1735.75 and 1673.63 cm^{-1}, as shown in Figure 9. By 55 °C, three peaks can be observed at 1735.29, 1706.98, and 1674.36 cm^{-1}. The new peak at 1706.98 cm^{-1} may be due to the partial loss of one water molecule (either (2) or (3)), changing the local environment of the carbonyl. By 60 °C the highest of these is lost and a shoulder appears on the band, at 1674.36 cm^{-1}. This band moved to 1683.45 cm^{-1} between 60 and 115 °C and eventually developed into the doublet characteristic of the α-form.

In the initial room temperature spectrum for the dihydrate there are two O−H bands at 3549.36 and 3470 cm^{-1}, corre-

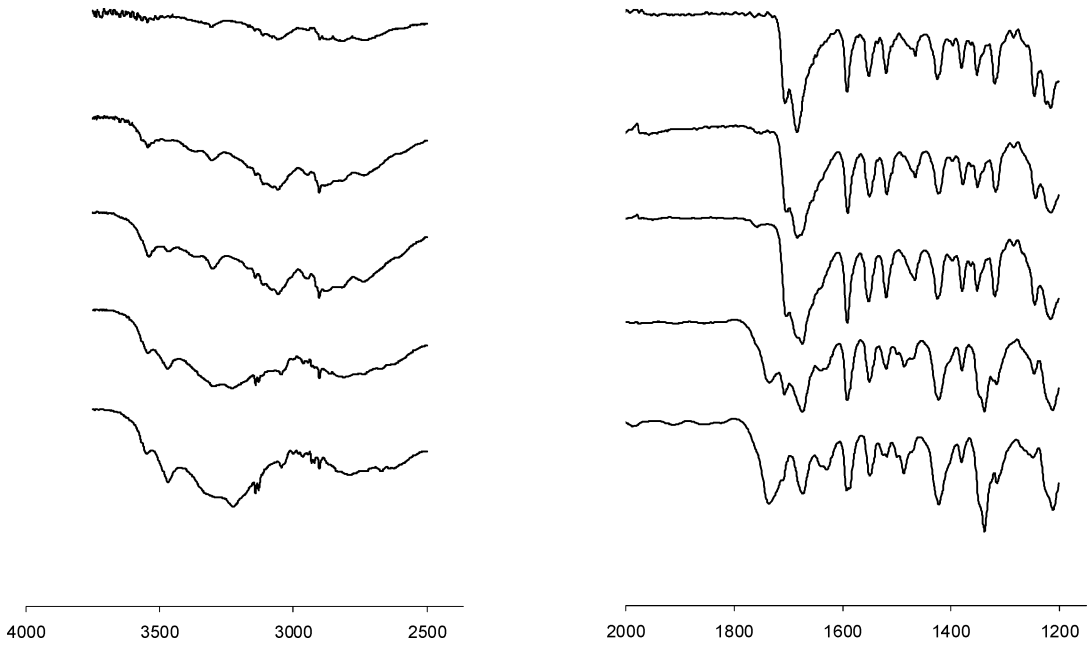

Figure 9. FT-IR spectra showing thermal dehydration of inosine dehydrate (from bottom: 32, 55, 60, 115, and 36 °C; horizontal axis in cm^{-1}).

sponding to lattice bound water molecules. By 55 °C these are found at 3534.00 and 3471.45 cm^{-1}, at 60 °C they are still present at 3539.35 and 3457.18 cm^{-1}, but by 115 °C there is only one band at 3545.50 cm^{-1}, close to the expected position in the α-form.

The results obtained from the variable temperature FT-IR study correspond well with those obtained from the hot stage PXRD experiments, in that intermediate structures are observed.

Solid State ^{13}C NMR. Solid state ^{13}C NMR spectra of the three forms (not shown) revealed significant differences in an in situ heating experiment. While at 40 °C the spectrum was identical to that of the dihydrate, by 55 °C the spectrum obtained was that of the α-form. In a sample held isothermally at 51 °C new peaks of the α-form began to appear, while the peaks of the dihydrate decreased in intensity. Unlike the PXRD and FT-IR results, but similar to the humidity experiments, there was no evidence for the formation of any intermediate forms—the sample analyzed by solid state NMR appeared to transform directly from dihydrate to the α-form.

Dynamic Vapor Sorption Study. The results obtained from DVS experiments correspond well with those obtained from the humidity PXRD experiments. The humidity was decreased from 45% to 0% in 15% steps. No significant weight loss was observed until 0%. When the humidity was increased, there was no increase in the weight of the sample, showing that once the sample has been dehydrated it transforms to an anhydrous form and cannot be rehydrated.

Discussion

Overall, it should be noted that the structural interpretation of the experimental data given below assumes that structure and kinetics may be treated independently and hence that the former may be understood without having to fully characterize the latter. Such an assumption seems to be justified on the basis of the optical microscopy, which shows no evidence for preferential surface dehydration of crystals, and PXRD, which shows that there are no apparent kinetic limitations to full dehydration of dihydrate samples. Thus, for example, when a sample is dehydrated by heating in air, as in the PXRD and FT-IR experiments, the water is quickly driven off and is no longer in contact with the inosine, there is evidence for the dehydration to proceed via structural intermediate forms and the final solid is transformed fully to α. When the sample is dehydrated in a humid atmosphere, as in environmental PXRD or the closed NMR cell, then water vapor is in contact with the solid phase and this appears to catalyze the transformation from the dihydrate directly to the α-form with no evidence of intermediate structures. Such catalysis is known in the solid state transformation between forms III and IV of ammonium nitrate,[21] where water facilitates structural rearrangement at the interface between the two forms. A similar situation may be true here, particularly as optical microscopy shows that one form (α) grows within the other.

If the dehydration is considered on the basis of the crystallographic packing in the three forms, then the graph sets (Table 2) suggest that the dihydrate would have transformed to the *β*-structure, not only because this is the more stable of the two polymorphs but also because of the common C1,1(5) N−H···N chain. This is the only common structural motif between dihydrate and either of the polymorphs. However, on reexamining the structures in the light of the experimental data, an alternative view is evident.

The four water molecules (see Figure 4) can be separated into two groups [(1) and (4), and (2) and (3)] determined by their location in the structure. Water molecules (2) and (3) form one hydrogen bond to each other and to the carbonyl group on each inosine conformation. This leads to the formation of a tetramer unit (see Figure 10a) in which the inosine molecules are connected not only through the two water molecules, but also through H-bonds from the −OH on the ring of one conformation to an N-atom on the other conformer. Each tetramer unit is linked to an adjacent one through H-bonds from the $-CH_2OH$ group to an N-atom on the neighboring unit. This leads to the formation of stacks of tetramers along the crystallographic *c*-axis (see Figure 3c). These stacks are then connected to each other along the *b*-axis through the five-membered N−H···N chains and along the *a*-axis by pairs of hydrogen bonded water molecules (1) and (4).

By now removing water molecules, insight may be obtained concerning possible structural rearrangements on dehydration

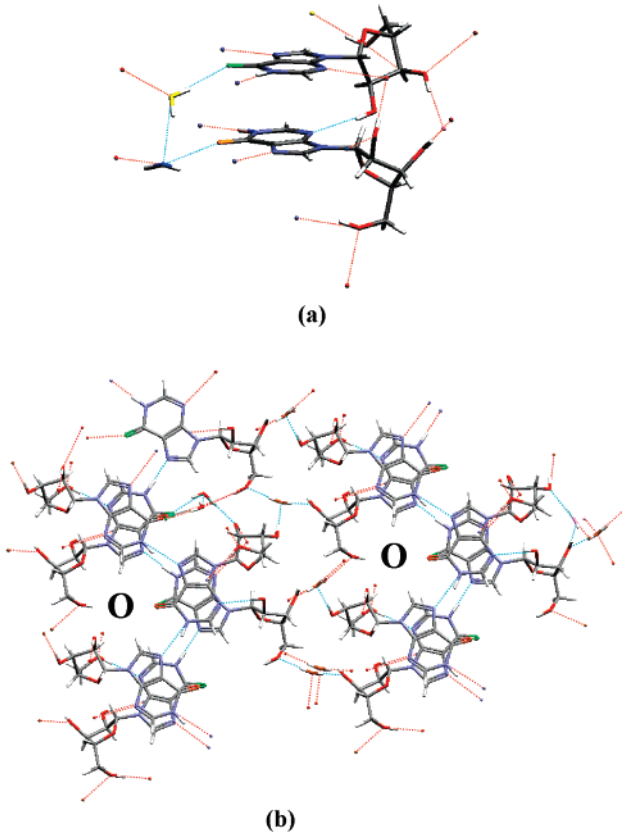

Figure 10. (a) Tetramer unit (green, C═O conformation 1; orange, C═O conformation 2; yellow, water (2); purple, water (3)). (b) Inosine dihydrate with three water molecules removed, showing the channels formed by loss of water (O) and viewed down *c*.

and a comparison made with the experimental data. For example, on removal of all environment 5 waters [(1), (2), and (3) in Figures 3c and 4] a channel, having a diameter of 4.1 Å (measured from O−H···O═C), appears within the structure seen in Figure 10b. This would predict that water molecule (4) would be lost last as it is an environment 6 water and would be the most tightly bound. In fact, as can be seen in Figures 3c and 4, the earlier loss of water (1) means that water (4) would actually be in environment 5 as the dehydration proceeds and still therefore held tightly in place.

This mechanism is consistent with the measurements. TGA, for example, indicates that water loss is indeed a two-stage process. More details of this may be discerned from PXRD and FT-IR. From the hot stage PXRD, we know that during the first stages of dehydration, when the first unique patterns are observed, the (100) reflection shifts by up to 1° from 5.088° to 5.876° 2θ, a contraction from 17.241 to 15.0 Å. Since this peak corresponds to the water-rich channel between the furan ends of the molecules, this suggests that one of the first structural changes is indeed the loss of water molecule (1) and contraction of the channel. Hot stage FT-IR shows that one of the first changes to take place upon dehydration is in the environment of the carbonyl ligand. This confirms that the waters (2) and (3), between the aromatic planes (see Figure 3c), are indeed being lost at an early stage in the dehydration process. The evidence from the PXRD and the FT-IR experiments therefore suggest the early loss of water molecules (1), (2), and (3). The next step in the process involves the conformational and packing changes needed for the transformation to the α-structure. The final α-packing is constructed from dimers in which one of the aromatic rings is rotated through 180° compared to the dihydrate structure. One possibility is that the channel formed upon the loss of water molecules (1), (2), and (3) allows both rotation of the furan rings and molecular translation. Consideration of Figure 3b shows that, for molecule 1, rotation of the furan ring to the left, into the β-conformation, is likely to be sterically hindered by the molecules in the layers above and below, while rotation to the right, to the α-conformation, is more accessible. This appears to be the key to the unexpected formation of the metastable α-structure. The void space adjacent to the carbonyl groups may then permit translation of the inosine molecules and subsequent weakening of the N−H···N interaction preventing formation of the β-structure. Alternate layers in the structure must then translate in opposite directions. This corresponds to the molecules in the (0 0 1) plane translating, for example, along the +*c*-axis while the molecules in the (0 0 2) plane translate in the opposite direction along the −*c*-axis.

The impact of humidity on this process may be to mediate these molecular rearrangements both at the crystal surface and at the interfacial region within the crystal. This would obviate the need for intermediate structural states.

Conclusions

This work has demonstrated the use of a powerful combination of analytical tools in the study of a dehydration process. In particular we have shown how, in the case of inosine dihydrate, these data may be used far beyond mere characterization to answer some key questions about the structural mechanisms taking place. In this case it has been possible to assign a two-stage mechanism in which the initial loss of three water molecules causes a channel to open, around which the final conformational and packing changes can proceed. The geometric restrictions that this implies, unexpectedly, give rise to the formation of the metastable polymorph. It is clear that the presence of water vapor is able to facilitate these processes.

References and Notes

(1) Stahl, H. P. In *The Problems of Drug Interactions with Excipients*; Braimer, D. D., Ed.; Elsevier/North-Holland Press: New York, 1980.
(2) Gillon, A. L.; Feeder, N.; Davey, R. J.; Storey, R. *Cryst. Growth Des.* **2003**, *3*, 663−673.
(3) Garner, W. E. *Chemistry of the Solid State*; Garner, W. E., Ed.; Academic Press: New York, 1955.
(4) Li, Y. H.; Han, J.; Zhang, G. G. Z.; Grant, D. J. W.; Suryanarayanan, R. *Pharm. Dev. Technol.* **2000**, *5*, 257.
(5) Chen, L. R.; Young, V. G.; Lechuga-Ballesteros, D.; Grant, D. J. W. *J. Pharm. Sci.* **1999**, *88*, 1191−1200.
(6) Leung, S. S.; Padden, B. E.; Munson, E. J.; Grant, D. J. W. *J. Pharm. Sci.* **1998**, *87*, 508−513.
(7) Perrier, P. R.; Byrn, S. R. *J. Org. Chem.* **1982**, *47*, 4671−4676.
(8) Stephenson, G. A.; Groleau, E. G.; Kleemann, R. T.; Xu, W.; Rigsbee, D. *J. Pharm. Sci.* **1998**, *87*, 536−541.
(9) Byrn, S. R.; Lin, C. T. *J. Am. Chem. Soc.* **1976**, *98*, 4004−4005.
(10) de Matas, M.; Edwards, H. G. M.; Lawson, E. E.; Shields, L.; York, P. *J. Mol. Struct.* **1998**, *440*, 97−104.
(11) Te, R. L.; Griesser, U. J.; Morris, K. R.; Byrn, S. R.; Stowell, J. G. *Cryst. Growth Des.* **2003**, *3*, 997−1004.
(12) Willart, J. F.; Danede, F.; De Gusseme, A.; Deschamps, M.; Neves, C.; *J. Phys. Chem. B* **2003**, *107*, 11158−11162.
(13) Petit, S.; Cocquerel, G. *Chem. Mater.* **1996**, *8*, 2247−2258.
(14) Munns, A. R. I.; Tollin, P.; Wilson, H. R.; Young, D. W. *Acta Crystallogr.* **1970**, *B26*, 1114−1117.
(15) Munns, A. R. I.; Tollin, P. *Acta Crystallogr.* **1970**, *B26*, 1101−1113.
(16) Subramanian, E. *Cryst. Struct. Commun.* **1979**, *8*, 777−785.
(17) Suzuki, Y. *Bull. Chem. Soc. Jpn.* **1974**, *47*, 2549−2550.
(18) Etter, M. C.; Macdonald, J. C.; Bernstein, J. *Acta Crystallogr.* **1990**, *B46*, 256−262.
(19) Bernstein, J.; Davis, R. E.; Shimoni, L.; Chang, N. L. *Angew. Chem., Int. Ed. Engl.* **1995**, *34*, 1555−1573.
(20) Allen, F. H. *Acta Crystallogr.* **2002**, *B58*, 380−388.
(21) Davey, R. J.; Ruddick, A. J.; Guy, P. D.; Mitchell, B.; Maginn, S. J.; Polywka, L. A. *J. Phys. D: Appl. Phys.* **1991**, *24*, 176−185.